Asian Journal of Chemistry; Vol. 25, No. 1 (2013), 245-250

ASIAN JOURNAL OF CHEMISTRY

http://dx.doi.org/10.14233/ajchem.2013.12919

Relationship Between the Doping Levels and Some Physical Properties of SnO_2:Sb Thin Films Spray-Deposited on Optical Glass

GÜVEN TURGUT*, DEMET TATAR and BAHATTIN DÜZGÜN

Department of Physics, K.K. Education Faculty, Ataturk University, Erzurum 25240, Turkey

*Corresponding author: Fax: +90 44 22369055; Tel: +90 44 22314011; E-mail: guventurgut@atauni.edu.tr

(*Received*: 24 October 2011; *Accepted*: 20 July 2012) AJC-11856

SnO_2:Sb thin films were prepared by the spray pyrolysis technique on optical micro slide glass at substrate temperature 793 (± 5) K. The relationship between the antimony doping level and the electrical, structural and optical properties of the films were investigated. The X-ray diffraction patterns showed that the films are polycrystalline. The grain size varies from 28.19 to 33.59 nm. Atomic force microscopic study revealed the surface of SnO_2:Sb to be made of nanocrystalline particles. The electrical study has revealed that the films are degenerate and exhibit *n*-type electrical conductivity. The SnO_2:Sb films had a minimum resistivity of 0.28×10^{-4} Ω cm, maximum carrier density of 37.6×10^{19} cm^{-3} and mobility of 590 cm^2/V.s. The sprayed SnO_2:Sb film having minimum sheet resistance of 0.17 Ω/cm^2, highest figure of merit of 135×10^{-4} Ω^{-1} at 550 nm. The sheet resistance attained for the doped film in this study has been lower than the values reported for 2 wt % antimony doped tin oxide films prepared from aqueous solution of $SnCl_2 \cdot 2H_2O$ precursor. The obtained results revealed that the structures and properties of the films were greatly affected by doping levels.

Key Words: SnO_2: Sb; X-ray diffraction, Spray pyrolysis, Thin films.

INTRODUCTION

In recent years, there has been a growing interest in the use of transparent conducting oxide thin films as transparent conducting layer in thin film solar cells[1,2], heat reflectors and as various gas sensors[3-6]. Tin oxide is the first transparent conductor to have received significant commercialization[1,7]. Among the different transparent conductive oxides, SnO_2 (TO) films seem to be the most appropriate for use in solar cells, owing to its low electrical resistivity (10^{-3} Ω cm) and high optical transmittance (90 %). Tin oxide is wide band gap (~4 eV) and indirect band gap (of about 2.6 eV) non-stoichiometric semiconductor[8]. Also, SnO_2 is chemically inert, mechanically hard and can resist high temperature[1]. The physical properties of SnO_2 films can be enhanced by doping with appropriate doping such as antimony (Sb), indium (In) and fluorine (F)[9,10]. Doped or undoped SnO_2 thin films can be synthesized by numerous techniques such as chemical vapour deposition (CVD)[11], sputtering[12], sol-gel process[13], spray pyrolysis[14,15], hydrothermal method[16] and pulsed laser deposition[17]. Among the various deposition techniques the spray pyrolysis is the well suited for the preparation of doped tin oxide thin films because of its simple and inexpensive experimental arrangement, ease of adding various doping material, reproducibility, high growth rate and mass production capability for uniform large area coatings, which are desirable for industrial and solar cell applications[1,6,10].

In the present work, SnO_2:Sb thin films have been prepared by the spray pyrolysis (SP) technique at substrate temperature of 793 K using dehydrate stannous chloride ($SnCl_2.2H_2O$ with 98 % purity, Merck) and antimony trichloride ($SbCl_3$ with 99 % purity, Merck) as precursors. The aim of this work is to study the relationship between the doping levels and some physical properties of SnO_2:Sb thin films such as the electrical and structural properties. The results obtained has been compared and discussed with the specified results by several researchers.

EXPERIMENTAL

The antimony doped tin oxide thin films reported in the present study were prepared using a homemade spray pyrolysis apparatus. The normalized distance between the spray nozzle and the substrate is 40 cm the spray angle (α) is 45º. The optimization was conducted by taking different sets of readings, keeping the nozzle to substrate distance as 25, 30, 35, 40 and 45 cm. A schematic diagram of this set-up and a detailed description of the deposition process have been given in Fig. 1. Thin films of SnO_2:Sb (ATO) were deposited on optical glass substrate ($75 \times 25 \times 1$ mm^3) by spray pyrolysis technique. Stannous chloride ($SnCl_2.2H_2O$ with 98 % purity, Merck) was used in making the precursor solution for SnO_2 thin films. Though $SnCl_2.2H_2O$ can partly ionize into Sn^{2+} and Cl^-, it could

also from tin based polymer molecules. 10 g of $SnCl_2.2H_2O$ dissolved in 5 mL of concentrated hydrochloric acid (HCl) was heated at 90 ºC for 10 min. The addition of HCl was required in order to break down the polymer molecules that were formed when diluting with methanol. This mixture was diluted by adding methanol served as starting solution and the diluted solution was made up to 25 mL. For antimony doping, antimony trichloride ($SbCl_3$ with 99 % purity, Merck) dissolved in isopropyl alcohol (25 mL) was added to the starting solution, in such a way as to result in antimony doping in the range of 0-4 wt. %, at the interval of 1 wt. %. Hence, antimony doped SnO_2 films were also deposited by means of varying doping antimony in the starting solution from 0 to 4 wt. %. [$SbCl_3$]/[$SnCl_2.2H_2O$] = 0, 1, 2, 3, 4 wt. %, respectively]. In each case, the amount of spray solutions prepared was 50 mL. All the spray solutions were magnetically stirred for 1 h and finally these solutions were filtered by syringe filter with 0.2 µm pore size before spraying on substrate. The microscopic glasses with 75 mm × 25 mm × 1 mm dimesions were used as subtstates. The substrates were washed with water, then boiled in concentrated chromic acid and kept in distilled water for 48 h and finally substrates were cleaned with organic solvents and helping ultrasonic cleaner. The substrates were pre-heated to the required temperature. The flow rate (1.25 mL/min), total spraying quantity (50 mL) and plate rotation speed (20 rpm) were all kept fixed. Filtered compressed air was used as carrier gas. The flow rate of air used as a carrier gas is about 1.25 mL/min. The total deposition time was maintained at 40 min for each film. The substrate temperature (working temperature) was 793 ± 5 K. The substrate temperature was maintained using a k-type thermocouple based on digital temperature controller. Uniform coating was achieved by rotating the substrate with a speed of 20 rpm in its plane. The samples were produced simultaneously at substrate temperature 793 (± 5) K. After deposition, the coated substrates were allowed to cool down naturally to room temperature. In each process, more than ten samples were produced simultaneously at each doping levels. It was realized that the crystals have similar properties and then passed to other processes.

The structural characterization of the films was carried out by X-ray diffraction measurements using a Rigaku Miniflex II diffractometer with CuK_α radiation (λ = 1.5418 Å), at 30 kV, 10 mA. Surface morphology of the resulting films was examined by SEM (Nova Nanosem 430) and atomic force microscopy (AFM), which was produced by nanomagnetics-instrument. The electrical measurements were carried out by Hall measurements at the room temperature. Optical transmittance measurements of the SnO_2:Sb films were measured using UV-VIS spectrophotometer (Perkin Elmer, Lambda 35) in the wavelength ranging from 400 to 1000 nm.

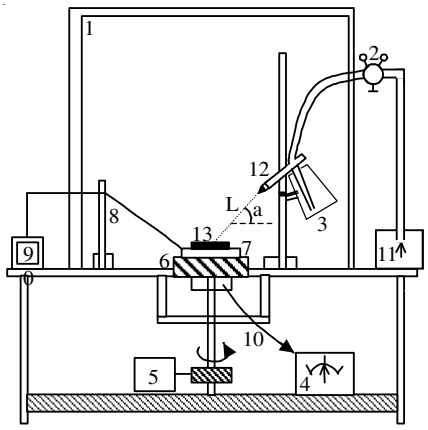

Fig. 1. Diagram of the apparatus used for spraying of doped SnO_2

RESULTS AND DISCUSSION

Structural properties: The surface morphology of the films was also studied by atomic force microscopy. The atomic force microscopy surface 2D images optained for SnO_2:Sb films prepared with different antimony doping concentrations are shown in Fig. 2. The smaller grains was appeared on the surface, once the antimony doping has commenced. The number of smaller grains increased with the increase in Sb doping. The triangular grains can be seen almost all over the substrate. The distribution of grains is uniformly on the substrate surface. The root mean square (RMS) values of surface roughness is found to be 100.27 to 257.19 nm for Sb doped film. The root mean square roughness of the films doped with 3 wt. % Sb is the lowest in comparision with other films (Table-1). Fig. 3(a)-(e) show 3D atomic force microscopy images of undoped and (from 0 wt. % to 1 wt. %) Sb-doped SnO_2 films and Fig. 3(f), the surface roughness variations of SnO_2:Sb films as a function of the doping levels. As the doping levels increased from 0 wt % to 1 wt %, the roughness of the films increased from 164.67 to 257.19 nm, after decreased to 100.27 nm and later increased to 112.87 nm. Detailed atomic force microscopy study reveals that the roughness of the film is dependent on the dopant concentration. The similar tendency has been observed by Elengovan *et al.*[9]. From atomic force microscopy images, it was observed that the grain size become larger with 1 and 2 wt. % Sb content, then become the small at 3 wt. % Sb and again become larger at 4 wt. % Sb concentration. These results resemble the results of Lee *et al.*[6].

TABLE-1
STRUCTURAL PROPERTIES OF ATO FILMS WITH DIFFERENT Sb-DOPING CONCETRATION

Sample	FWHM	D (nm)	RMS (nm)	δ (× 10^{14} lines/m^2)
0 % wt. Sb (301)	0.321	30.77	164.67	10.56
1 % wt. Sb (211)	0.296	31.13	257.19	10.32
2 % wt. Sb (301)	0.318	31.03	166.07	10.39
3 % wt. Sb (301)	0.350	28.19	100.27	12.58
4 % wt. Sb (200)	0.261	33.59	112.87	8.86

FWHM- Full width at half maximum, D-Crystallite size; RMS- Root mean square roughness; δ-dislocation density

The XRD patterns recorded for SnO_2:Sb thin films deposited by the spray pyrolysis technique as function the doped levels are shown in Fig. 4. Films deposited at different concentration caused further healing of the crystallization of the films as mentioned by other researchers[11,18]. Since all the peaks are sharp it is evident that the films with different antimony doping levels are polycrystalline in nature and are of cassiterite tetragonal structure. The pure tetragonal SnO_2 films have strongest (301) planes, but for 1 wt. % Sb doped film

slight change (211) prefered orientation. For films with antimony doping concentrations of 2 and 3 wt. %, this strongest preference oriantation is (301). For films with antimony doping concentrations of 4 wt. %, this strongest preference oriantation is (200). A similar tendency for (200), (110) and (101) texture was found in SnO_2:Sb films when a starting solution of $SnCl_2$ in HCl was employed[7]. This means (in our opinion) that the preferential orientations of crystal growth are strongly dependent on doping concentration.

The film thickness of SnO_2 films doped was estimated to be 1.66 μm by cross-sectional SEM images. The SEM micro graphs displaying the surface morphology of SnO_2:Sb films are shown in the Fig. 5 for the different levels of antimony doping. The undoped film is characterized by uniform-sized grains with triangular shape in the doped films. The smaller grains started appearing on the surface. The number of smaller grains increased with the increase in Sb doping. The needle shaped grains has appeared on the surface of antimony-doped films (4 wt.%) for those having preferred orientation along (200) plane. For the film doped with 2 wt.% of Sb, the needle shaped grains were found absent. The same difference in orientation has been reflected in SEM studies as they lead to different grain shapes. The grain size of SnO_2:Sb films deposited with different doping levels is calculated us ing Scherrer's formula[9], $D = 0.9\ \lambda/(\beta \cos\theta)$ where D is the size of crystallite,

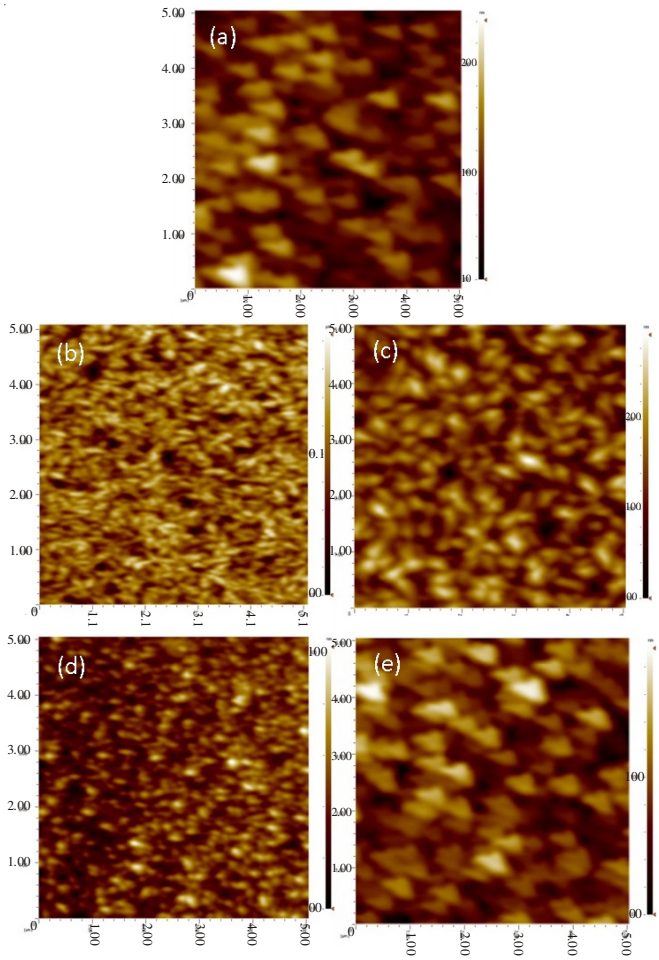

Fig. 2. AFM surface (5 mm × 5 mm) 2D images obtained for SnO_2:Sb prepared with different antimonydoping levels: (a) 0 wt. %, (b) 1 wt. %, (c) 2 wt. %, (d) 3 wt. %, (e) 4 wt. % respectively

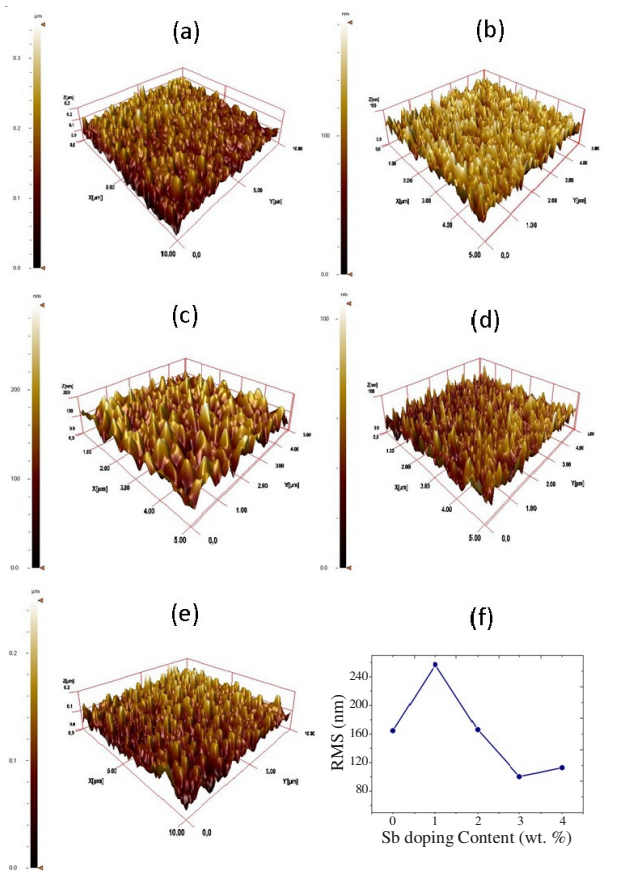

Fig. 3. AFM surface 3D images of SnO_2:Sb films as a function of Sb-doping concentration: (a) 0 wt. %, (b) 1 wt. %, (c) 2 wt. %, (d) 3 wt. %, (e) 4 wt. %, (f) the surface RMS roughness variation of SnO_2:Sb films as a function af Sb-doping concentration

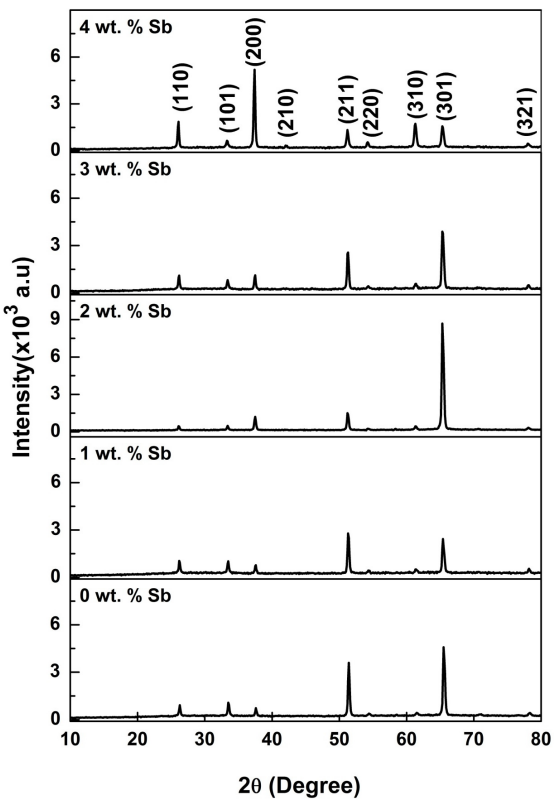

Fig. 4. XRD spectra of the SnO_2:Sb films deposited on glass at different concentration

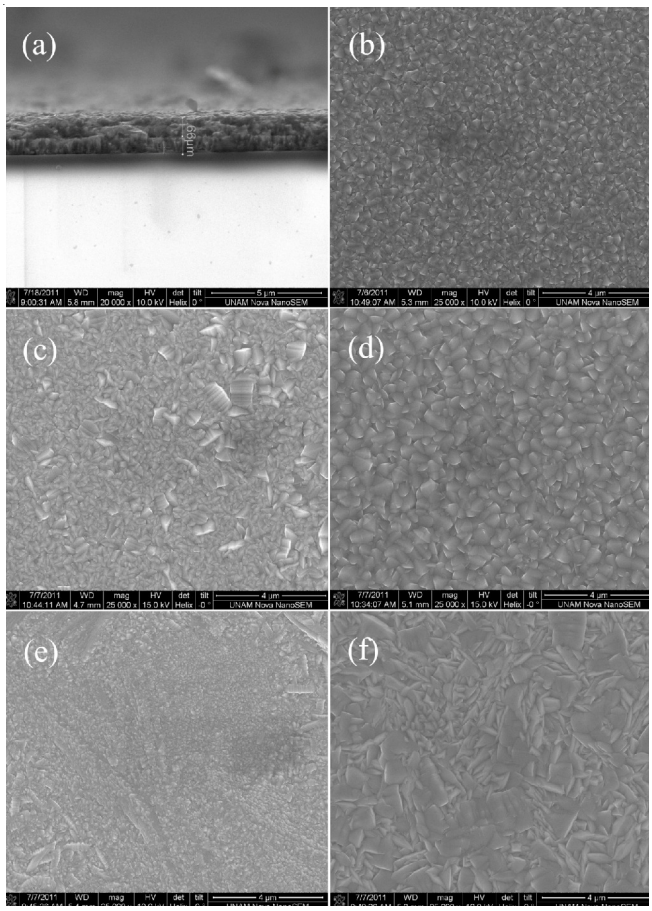

Fig. 5. SEM micrographs SnO_2:Sb films obtained for different deposition concentration [(a) Cross-sectional, (b) 0 wt. %, (c) 1 wt. %, (d) 2 wt. %, (e) 3 wt. %, (f) 4 wt. %, respectively]

β is the broadening of diffraction line measured at half its maximum intensity in radians and λ is wavelength of X-rays (λ = 1.5418 Å). The calculated values of grain size are given in Table-1. Grain size variation of SnO_2:Sb films as a function of the doped levels was shown in Fig. 6. It may be seen that the grain size changed more slowly, before increase (from 0 wt. % to 2 wt. %), then decrease (up to 3 wt. %) then quickly increase (up to 4 wt. %) with increase antimony doping. As seen, there are similarity between SEM images and grain size. This indicates that the grain size of the film is dependent on dopant concentration. Such a discrepancy in grain size values has been reported by several researchers[19,20].

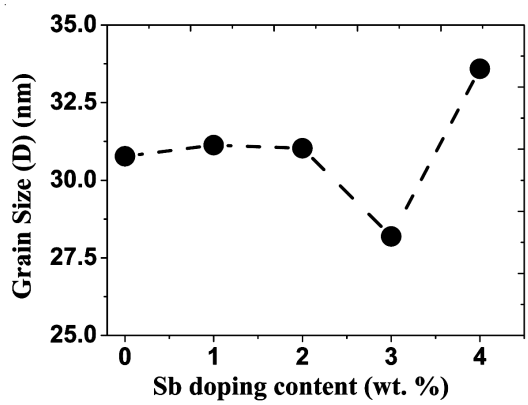

Fig. 6. Grain size of various deposition concentration in SnO_2:Sb films

The lattice constant a and c, for the tetragonal phase structure are determined by the relation $(1/d^2) = \{[(h^2+k^2)/a^2] + (l^2/c^2)\}$, where d is the interplaner distance and (hkl) are miller indices, respectively. The calculated lattice constant a and c were given in Table-2. The lattice constants a and c calculated compared with the standard JCPDS data card no. 41-1455.

TABLE-2
STRUCTURAL PARAMETERS OF ATO THIN FILMS WITH DIFFERENT DOPING CONCENTRATION

Sample	(hkl)	dst(Å)	dobs(Å)	a(Å)	c(Å)
0 wt. % Sb	110	3.3470	3.3876	4.7624	3.1851
	101	2.6427	2.6706		
	200	2.3690	2.3894		
	211	1.7641	1.7760		
	220	1.6750	1.6847		
	310	1.4984	1.5060		
	301	1.4155	1.4232		
1 wt. % Sb	110	3.3470	3.3945	4.7703	3.2150
	101	2.6427	2.6747		
	200	2.3690	2.3917		
	211	1.7641	1.7785		
	220	1.6750	1.6851		
	310	1.4984	1.5085		
	301	1.4155	1.4253		
	321	1.2147	1.2212		
2 wt. % Sb	110	3.3953	3.4059	4.7757	3.1762
	101	2.6748	2.6797		
	200	2.3690	2.3965		
	211	1.7795	1.7812		
	220	1.6854	1.6892		
	310	1.5099	1.5102		
	301	1.4257	1.4268		
	321	1.1919	1.2225		
3 wt. % Sb	110	3.3470	3.4020	4.7722	3.1879
	101	2.6427	2.6798		
	200	2.3690	2.3977		
	211	1.7641	1.7800		
	220	1.6750	1.6881		
	310	1.4984	1.5091		
	301	1.4155	1.4268		
	321	1.2147	1.2224		
4 wt. % Sb	110	3.3470	3.4141	4.7782	3.1842
	101	2.6427	2.6869		
	200	2.3690	2.4027		
	210	2.1189	2.1459		
	211	1.7641	1.7823		
	220	1.6750	1.6905		
	310	1.4984	1.5110		
	301	1.4155	1.4271		
	321	1.2147	1.2235		

The growth mechanism involving dislocation is matter of importance. Dislocations are imperfect in a crystal associated with the mis-registry of the lattice in one part of the crystal with respect to another part. Unlike vacancies and interstitials atoms, dislocations are insufficient to account for their existence in

the observed dislocation densities[21-23]. The dislocation density (δ), defined as the length of dislocation lines per unit volume. Since δ is the measure of the amount of defects in a crystal. The dislocation density (δ) was determined using the relation $\delta = 1/D^2$ [21,24]. For SnO_2:Sb thin films these values are the calculated structural parameters are summarized in Table-1.

Electrical properties: The electrical measurements were carried out by Hall measurements at the room temperature. The negative sing of Hall coefficient confirmed the *n*-type conductivity of the films. Fig. 7 shows resistivity (ρ), mobility (μ) and carrier concentration (n) of SnO_2:Sb films as a function of the doping levels. The results were also given in Table-3. The values of μ, n and ρ are obtained from the combined measurements of resistivity and Hall coefficient. As seen in the table, there is a rapid decrease of the resistivity to 2 wt. % Sb doping level. When the doping levels is increased from 2 wt. % to 4 wt. %, the resistivity (ρ) increases again. Hall mobility (μ) and carrier concentration (n) were also measured and the results were included in the same table. When the doping levels have been increased from 0 wt. % to 2 wt. % mobility and carrier concentration have been increased from 356 to 590 $cm^2 V^{-1} s^{-1}$; from 0.66×10^{19} to 37.6×10^{19} cm^{-3}, respectively. After, the carrier concentration have been decreased up to 4 wt. % Sb content. The variation in the sheet resistance of tin oxide thin films with antimony doping can be explained on the basis of the presence of Sb in two oxidation states, Sb^{5+} and Sb^{3+}. When SnO_2 is doped with Sb, some of the Sn^{4+} ions in the lattice are replaced by Sb^{5+}, resulting the sheet resistance[7]. Hence, a continuous reduction in the sheet resistance was observed until the Sb concentration reaches 2 wt.%. Beyond 2 wt. % of Sb doping, a part of the Sb^{5+} ions is reduced to the Sb^{3+} state, resulting in the formation of acceptor states and a concomitant loss of carriers[7] and an increasing was observed at sheet resistance. Elengovan *et al.*[25] found minimum sheet resistance values of 2.17 Ω/cm^2 for 2 wt % antimony doped tin oxide films prepared from aqueous solution of $SnCl_2.2H_2O$ precursor. The minimum sheet resistance (0.17 Ω/cm^2) value for the 2 wt. % Sb doped film in this study is lower than the values reported for 2 wt % antimony doped tin oxide films prepared from aqueous solution of $SnCl_2.2H_2O$ precursor. This result may be caused by thicker film thickness than their films.

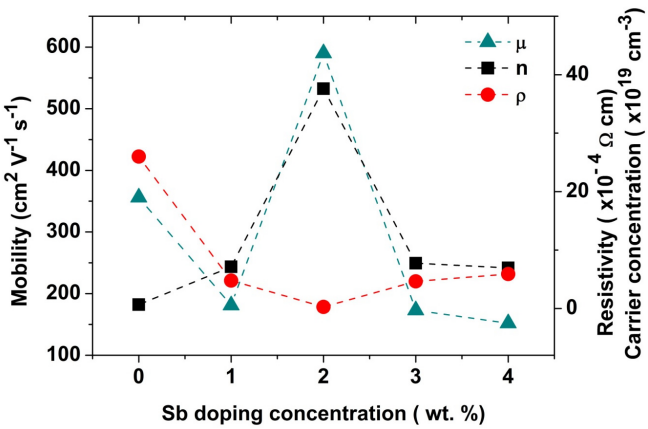

Fig. 7. Mobility, resistivity and carrier concentration of SnO_2:Sb films as a function of Sb Doping concentration

TABLE-3
ELECTRICAL PARAMETERS OF ATO THIN FILMS WITH DIFFERENT DOPING CONCENTRATION

Sample	Rs (Ω cm^{-2})	ρ (× 10^{-4} Ω cm)	μ (cm^2 /Vs)	n (× 10^{19} cm^{-3})
0 % wt. Sb	15.8	26.0	356	0.66
1 % wt. Sb	2.89	4.79	181	7.15
2 % wt. Sb	0.17	0.28	590	37.6
3 % wt. Sb	2.80	4.65	173	7.75
4 % wt. Sb	3.56	5.90	152	6.95

Sheet resistance (Rs), electrical resistivity (ρ), electron mobility (μ), free electron concentration (n)

Optical properties: Fig. 8 shows the variation of transmittance (T) with respect to wavelength of SnO_2:Sb thin films with different antimony doping levels. A minimum transmittance value of 48.44 % obtained for the 4 wt. % Sb doped film is increased to 64.19 % when the films are doped with 3 wt.% Sb (Table-4). A changing in transmission is observed with the increase in doping levels. These values are comparable with the values found in the literature[6,21]. The transmittance of pure tin oxide films is found to changed from 75.15 to 48.14 % (at 550 nm) on the addition of 4 wt. % of antimony (Fig. 8 and Table-4). As shown in, the transmittance is found to decrease if the antimony cocentration is increased above 0 wt. %. This suggests that the decrease in the transmittance of SnO_2:Sb films with increase in doping concentration may be due to the increasing absorption by free electrons. In general, in the visible region of the spectrum, the transmission is very high. It is due to the fact that the reflectivity is low and there is no absorption due to transfer of electrons from the valence band to the conduction band owing to optical interference effect, it is possible to maximize the transmission of thin film at particular region of wavelengths[21].

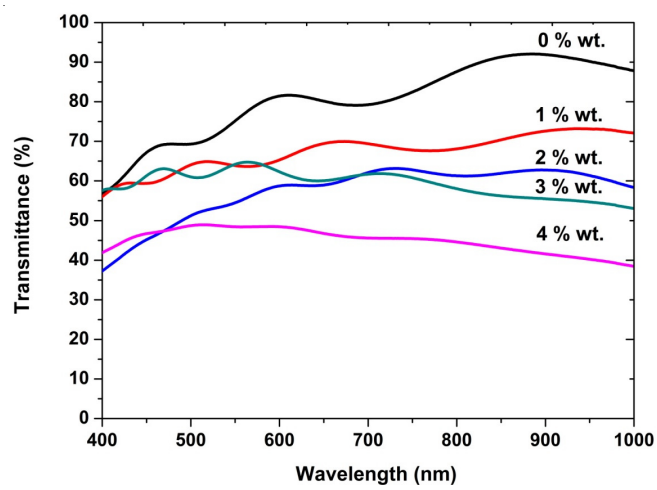

Fig. 8. Optical transmission spectra of SnO_2:Sb thin films as a function of Sb-doping concentration

The figure of merit is an important parameter for evaluating TCO thin films for use in solar cells[10]. Conductivity and transmittance are inversely proportional to each other and should be as possible for effective usage. In order to compare the performance of various transperent conductors the most widely used figure of merit as defined by Haacke is $\Phi_M = T^{10}/R_{sh}$[26], where T is the transmittance at 550 nm and R_{sh} is sheet

resistance. This formula gives more weight to the transparency and thus is better adapted to solar cell technology. It is clear that figure of merit is dependent on the sheet resistance. It is important to note that the figure of merit is also a function of the film thickness. Therefore, a thicker film will have a lower sheet resistance and which in turn will have higher figure of merit. The calculated figure of merit values are given in Table-4. It was found that the value obtained for the films doped with 2 wt. % Sb is the highest value obtained in present study ($135 \times 10^{-4}\ \Omega^{-1}$). This is possible due to formation of good quality of film in terms of coductivity and transmittance only at this deposition concentration. As step, the obtained values are in good agreement with the earlier reports[27-29].

TABLE-4
FIGURE MERIT FOR Sb DOPED SnO_2 THIN FILMS AT VARIOUS DEPOSITION CONCENTRATION

Sample	T (%) at 550 nm	Rs (Ω/cm^{-2})	ϕ ($\times 10^{-4}\ \Omega^{-1}$)
0 % wt. Sb	75.15	15.8	36.0
1 % wt. Sb	63.87	2.89	39.0
2 % wt. Sb	54.47	0.17	135
3 % wt. Sb	64.19	2.80	42.0
4 % wt. Sb	48.44	3.56	1.99

T- the transmittance at 550 nm; Rs-sheet resistance; ϕ - figure of merit

Conclusion

Polycrytalline thin films of SnO_2 with different ([Sb]/[Sn] ratios) antimony doping concentrations were prepared using a homemade spray pyrolysis apparatus at substrate temperatures 793 (± 5) K onto amorphous glasses. The effects of doping levels on structural, electrical and optical properties of SnO_2:Sb films were experimentally investigated. X-ray diffraction studies reveal that the material in the thin form is polycrystalline with tetragonal structure. The hall measurements show that the coductivity of the films is of *n*-type. The electrical coductivity characteristics, atomic force microscope images and X-ray difraction patterns that confirmed that the crystallinity effected with doping levels. The SnO_2:Sb films are very smooth. X-ray diffraction pattern revals the presence of cassiterite structure with (200), (211) and (301) preferential orientation for pure and Sb doped tin oxide films. The lowest sheet resistance (R_{sh}) for the SnO_2:Sb films was 0.17 Ω/cm^2. A high value of figure of merit (Φ) in the SnO_2:Sb films was $135 \times 10^{-4}\ \Omega^{-1}$ at 550 nm. All the films are degenerate with carrier concentrations (*n*) in the range of 0.66×10^{19}- $37.6 \times 10^{19}\ cm^{-3}$. The resistivities ($\rho$) and mobility ($\mu$) of the samples are of the order of 26×10^{-4}-$0.28 \times 10^{-4}\ \Omega$ cm; 152-590 cm^2/V.s., respectively. The obtained results are suggesting that the deposited films could be used as transparent electrodes in solar cells applications.

With this method, similar studies were made previously by many researchers, emphasized the similarities and differences between the results obtained. The sheet resistance attained (0.174 Ω/cm^2) for the doped film [prepared at 793 (±5) K] in this study is lower than the values reported for 2 wt % antimony doped tin oxide films prepared from aqueous solution of $SnCl_2.2H_2O$ precursor. In addition to other differences and similarities, these are the most important results obtained from the study.

REFERENCES

1. B. Thangaraju, *Thin Solid Films*, **402**, 71 (2002).
2. A. Goetzberger and C. Hebling, *Sol. Energy Mater. Cells*, **62**, 1 (2000).
3. J.R. Brown, P.W. Haycock, L.M. Smith, A.C. Jones and E.W. Williams, *Sens. Act. B*, **63**, 109 (2000).
4. P. Nelli, G. Faglia, G. Sberveglieri, E. Cerede, G. Gabetta, A. Dieguez and J.R. Morante, *Thin Solid Films*, **371**, 249 (2000).
5. I. Stambolova, K. Konstantinov and Ts. Tsacheva, *Mater. Cham. Phys.*, **63**, 177 (2000).
6. X.M. Mu, C.Y. Peng and C.L. Wu, *Asian J. Chem.*, **24**, 1554 (2012).
7. E. Elangovan, S.A. Shivashankar and K. Ramamurthi, *J. Cryst. Growth*, **276**, 215 (2005).
8. S.J. Ikhmayies and R.N. Ahmad-Bitar, *Mat. Sci. Semicond Proc.*, **12**, 122 (2009).
9. E. Elengovan and K. Ramamurthi, *Appl. Surf. Sci.*, **249**, 183 (2005).
10. N. Menarian, S.M. Rozati, E. Elemurugu and E. Fortunato, *Phys. Status Solid. C*, **9**, 2277 (2010).
11. K.S. Kim, S.Y. Yoon, W.J. Lee and K.H. Kim, *Surf. Coat. Technol.*, **138**, 229 (2001).
12. J. Ma, X. Hao, H. Ma, X. Xu, Y. Yang, S. Huang, D. Zhang and C. Cheng, *Solid State Commun.*, **121**, 345 (2002).
13. L.K. Dua, A. De, S. Chakraborty and P.K. Biswas, *Mater. Characterization*, **59**, 578 (2008).
14. T. Serin, N. Serin, S. Karadeniz, H. Sari, N. Tugluoglu and O. Pakma, *J. Non-Cryst. Solids*, **352**, 209 (2006).
15. K. Murakami, K. Nakajima and S. Kaneko, *Thin Solid Films*, **515**, 8632 (2007).
16. J. Zhang and L. Gao, *Mater. Chem. Phys.*, **87**, 10 (2004).
17. H. Kim and A. Pique, *Appl. Phys. Letts.*, **84**, 218 (2004).
18. P. Pajaram, Y.C. Goswami, D. Rajagopalan and V.K. Gupta, *Mater. Lett.*, **54**, 163 (2002).
19. K. Ravichandran, G. Muruganantham and B. Sakthivel, *Physca B*, **404**, 4299 (2009).
20. C.M. Shen, X.G. Zhang and H.L. Ll., *Appl. Surf. Sci.*, **240**, 34 (2005).
21. R.R. Kasar, N.G. Deshpande, Y.G. Gudage, J.C. Vyas and R. Sharma, *Physica B*, **403**, 3724 (2008).
22. A. Beltron and J. Andres, *Appl. Phys. Lett.*, **83**, 635 (2003).
23. M. Bedir, M. Öztas, O.F. Bakkaloglu and R. Ormanci, *Eur. Phys. J.*, **B45**, 465 (2005).
24. M. Dhanam, R. Balsundharprabhu, S. Jayakumar, P. Gopalkrishnan and M.D. Kannan, *Phys. Stat. Sol. (a)*, **19**, 149 (2002).
25. E. Elangovan, S.A. Shivashankar and K. Ramamurthi, *J. Cryst. Growth*, **276**, 215 (2005).
26. A.R. Babar, S.S. Shinde, A.V. Moholkar, C.H. Bhosale, J.H. Kim and K.Y. Rajpure, *J. Alloys Comp.*, **505**, 416 (2010).
27. E. Elangovan and K. Ramamurthi, *Thin Solid Films,* **476**, 231 (2005).
28. A.V. Moholkar, S.M. Pawara and K.Y. Rajpure, *J. Phys. Chem. Solids*, **68**, 1981 (2007).
29. K. Ravichandran and P. Philominathan, *J. Mater Sci: Mater. Electron.*, **22**, 158 (2011).